

Radiometric characteristics of new diamond PIN photodiodes

A BenMoussa¹, U Schühle², F Scholze³, U Kroth³, K Haenen^{4,5},
T Saito⁶, J Campos⁷, S Koizumi⁸, C Laubis³, M Richter³,
V Mortet⁴, A Theissen¹ and J F Hochedez¹

¹ Royal Observatory of Belgium, Circular Avenue 3, B-1180 Brussels, Belgium

² Max-Planck-Institut für Sonnensystemforschung, D-37191 Katlenburg-Lindau, Germany

³ Physikalisch-Technische Bundesanstalt (PTB), Abbestr. 2-12, D-10587 Berlin, Germany

⁴ Institute for Materials Research, Hasselt University, Wetenschapspark 1,
B-3590 Diepenbeek, Belgium

⁵ Division IMOMECE, IMEC vzw, Wetenschapspark 1, B-3590 Diepenbeek, Belgium

⁶ National Metrology Institute of Japan (NMIJ), 1-1-1, Umezono, Tsukuba,
Ibaraki 305-8563, Japan

⁷ Instituto de Física Aplicada (CSIC), Serrano 144, 28006 Madrid, Spain

⁸ Advanced Materials Laboratory, National Institute for Materials Science (NIMS),
1-1 Namiki, Tsukuba 305-0044, Japan

E-mail: ali.benmoussa@oma.be

Received 21 November 2005, in final form 7 February 2006

Published 23 March 2006

Online at stacks.iop.org/MST/17/913

Abstract

New PIN photodiode devices based on CVD diamond have been produced showing high responsivity in a narrow bandpass around 200 nm. A set of measurement campaigns was carried out to obtain their XUV-to-VIS characterization (responsivity, stability, linearity, homogeneity). The responsivity has been measured from the XUV to the NIR, in the wavelength range of 1 nm to 1127 nm (i.e. 1240 to 1.1 eV). The diamond detectors exhibit a high responsivity of 10 to 30 mA W⁻¹ around 200 nm and demonstrate a visible rejection ratio (200 nm versus 500 nm) of six orders of magnitude. We show that these PIN diamond photodiodes are sensitive sensors in the 200 to 220 nm range, stable under brief irradiation with a good linearity and homogeneity. They will be used for the first time in a solar physics space instrument LYRA, the Large Yield RAdiometer.

Keywords: UV detectors, diamond, photodiode

1. Introduction

LYRA, the Large Yield RAdiometer [1], is a solar VUV radiometer that will embark in 2007 onboard PROBA-2 (PRoject for On-Board Autonomy), a technologically oriented European Space Agency (ESA) micro-mission conceived for the purpose of demonstrating new technologies with prototype payloads. LYRA will monitor the solar irradiance in four selected UV passbands chosen for their relevance to solar physics, aeronomy and space weather: (1) the 200–220 nm Herzberg continuum range, (2) 121.6 nm corresponding to the H I Lyman- α wavelength, (3) the aluminium channel (17–70 nm) and (4) the zirconium channel (1–20 nm) where solar variability is highest. It will be the first space

assessment of a pioneering UV diamond detector program [2]. Diamond is a wide bandgap semiconductor ($E_g \cong 5.5$ eV at room temperature) which makes the sensors ‘solar-blind’: insensitive to the solar spectrum below the Earth’s atmosphere (at sea level) with a good UV/visible response ratio (e.g. more than four to five orders of magnitude). By using diamond detectors, the number of filters usually needed to block the unwanted visible radiation can be reduced and the serious attenuation of the desired UV radiation can be avoided. For the LYRA project, two types of diamond detectors are developed: photodiode (PIN) and photoconductor (MSM) detectors. In this paper, we report on the performance of the PIN devices only, while results on MSM photoconductor detectors have been reported in a previous publication [3].

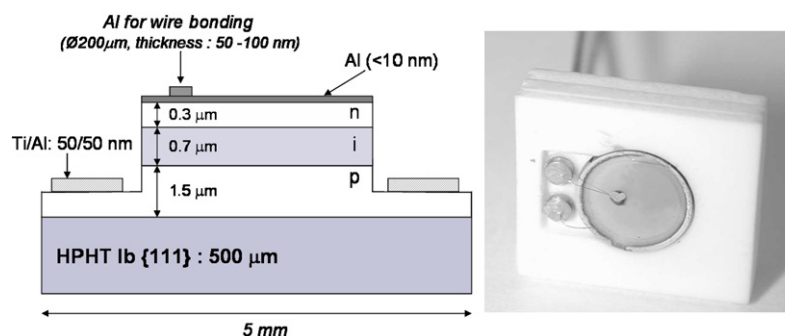


Figure 1. Schematic representation and photograph of the diamond PIN photodiode.

2. Experimental procedure

Several PIN photodiodes of circular shape have been fabricated for LYRA. The reported samples are designated PIN7, 11 and 12 in the LYRA project as well as throughout this paper. PIN detector structures were developed in a joint collaboration between IMO-IMOMECE in Belgium and NIMS in Japan. The homoepitaxial CVD layers of the detector were deposited in two different ULVAC stainless steel chamber plasma-enhanced microwave deposition reactors. Each apparatus is solely used for one type of doping, i.e. p-type (boron) or n-type (phosphorus), in order to avoid unwanted contaminations of the CVD diamond layers. After a careful selection and chemical oxidation of {111}-oriented, 5 mm diameter and 0.5 mm thick HPHT Ib diamond substrates from *Element Six*, an epitaxial p-type boron-doped layer is deposited. Boron doping is accomplished by adding trimethylboron (TMB) to the typical low-concentration methane-to-hydrogen mixture (CH_4/H_2) of 0.05%. Other typical process parameters are a pressure of 100 Torr, a substrate temperature around 900–950 °C and a microwave power of about 400 W. The intrinsic and phosphorus-doped n-type layers are grown in the same deposition run making use of the second growth apparatus. Starting with a normal CH_4/H_2 mixture for the intrinsic layer, phosphine (PH_3) is added to get an n-type layer. Compared to the first process, these layers are deposited at a slightly higher microwave power (700 W) and lower substrate temperatures (870–900 °C). In order to make an electrical contact with the B-doped layer, part of the intrinsic/P-doped layer needs to be removed using reactive ion etching (RIE). Therefore an Al disc (4.2 mm in diameter) is deposited on the top of the structure. This layer, acting as a mask during the RIE, is chemically removed afterwards. As a final step, two ohmic contacts are evaporated: Ti/Al (50/50 nm) for the p-type layer (ring), and a thin Al layer (<10 nm) with a transmittance of typically 20% to 50% for the top contact. A schematic representation and a photograph of the PIN detector mounted inside its rectangular ceramic package are shown in figure 1.

The synchrotron radiation campaign was carried out at the soft x-ray grazing incidence (GI) radiometry beamline (wavelength range 1 to 30 nm) and at the normal incidence (NI) beamline (40 to 240 nm) of the Physikalisch-Technische Bundesanstalt (PTB) laboratory at the storage ring Berliner Elektronenspeicherung-Gesellschaft für Synchrotronstrahlung (BESSY II). Details of the description of the PTB/BESSY II

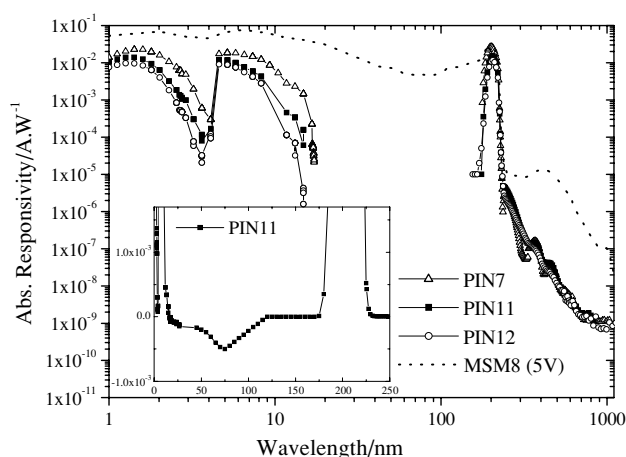


Figure 2. Absolute spectral responsivity (in A W^{-1}) of PIN7, 11, 12 (unbiased) and MSM8 at 5 V bias (dotted line) at room temperature between 1 nm and 1000 nm. The inset shows a close view of the linear scale of the negative photoresponse of PIN11.

measuring stations can be found in [4, 5]. For the longer wavelength range, monochromatic light is generated with a water cooled UV-enhanced 150 W Xe-lamp ($\lambda > 210 \text{ nm}$) or by a tungsten halogen lamp ($\lambda > 350 \text{ nm}$) at IMO-IMOMECE. A schematic representation of the setup can be found in [6].

3. Results and discussion

3.1. Absolute spectral responsivity

The absolute spectral responsivity curves at room temperature of PIN7, 11 and 12 are shown in figure 2. For comparison, we plotted the data of LYRA photoconductor MSM8 under 5 V bias [3]. Note that the PIN photodiode is operated in a photovoltaic mode (unbiased). The data from IMO-IMOMECE (210 nm to 1000 nm, measured on a relative scale) were matched to the absolute data from PTB/BESSY II (1 nm to 240 nm). For clarity, we did not plot the estimated error bars to the data points. A compilation of their contributions to the measurement uncertainties in the spectral responsivity is given in [7, 8].

The responsivity of the PIN detectors shows the diamond band edge to be around 225 nm and displays a UV/visible ratio (200 nm/500 nm) of six orders of magnitude. PIN detectors show a high responsivity around 200 nm of 27.2 mA W^{-1} for PIN7, 15.4 mA W^{-1} for PIN11 and 11.6 mA W^{-1} for PIN12.

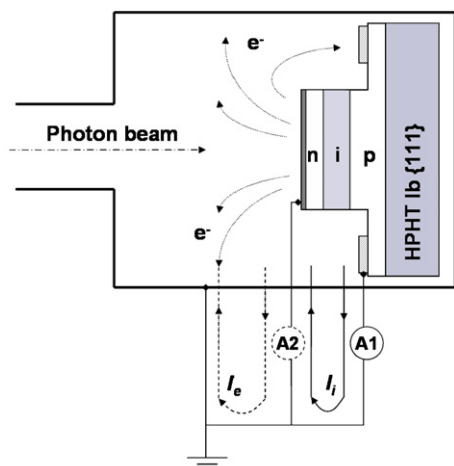


Figure 3. Schematic representation of the measurement configuration in the NI radiometry beamline. The photocurrent is measured in two electrical circuits (electrometer in position A1 then A2), I_i internal photocurrent and I_e external photoemission current.

It then decreases dramatically at higher energy due to the absorption of the n-type layer (surface and bulk recombination) associated with the abrupt drop of the diamond penetration depth which is around 20 nm at 170 nm wavelength and lower than 10 nm between 40 and 140 nm wavelengths [3]. Thus, electron-hole pairs are created very close to the surface and recombine before reaching the depletion region.

The responsivity becomes negative around 140 to 165 nm wavelength, depending on the devices, but with an extremum of approximately -0.5 mA W^{-1} at around 75 nm wavelength (see inset of figure 2). When going to higher energy, the responsivity starts to increase as observed for MSM photoconductors. It reaches positive values at about 15 nm. The responsivity, measured in finer steps around the carbon absorption edge at 4.4 nm (i.e. 284 eV), varies strongly (two orders of magnitude) depending on the device. At around 2 nm, the responsivity starts to decrease which can be related to the low atomic number ($Z = 6$) of diamond. This implies a small (capture) cross section, thus reducing the sensitivity of the detectors to higher energies (x- and γ -rays [9]).

The negative photoresponse should be seen in relation to the photoemission contribution [10, 11] which is significant in the same wavelength range (i.e. between 40 and 140 nm). A maximum photoemission yield at approximately 75 nm wavelength was measured for all PIN photodiodes. For a better understanding of the photoemission contribution, a schematic representation of the measurement configuration is shown in figure 3. The negative responsivity is explained by the fact that a proportion of the photoemitted electrons is collected directly at the p-contact (outer ring contact), which in turn is likely due to the proximity of that contact with the emitting surface (see in figure 1). This was confirmed by placing a metallic aperture in front of the PIN diode to collect the photoemitted electrons. When applying a bias of approximately 17 V to this aperture, we observed at 75 nm wavelength a change of the photoresponse's signal from negative to positive value (see figure 4). Moreover, we can see, in the inset of figure 4, the positive absolute spectral responsivity of PIN8 between 60 nm and 115 nm when applying a bias of 50 V to the metallic

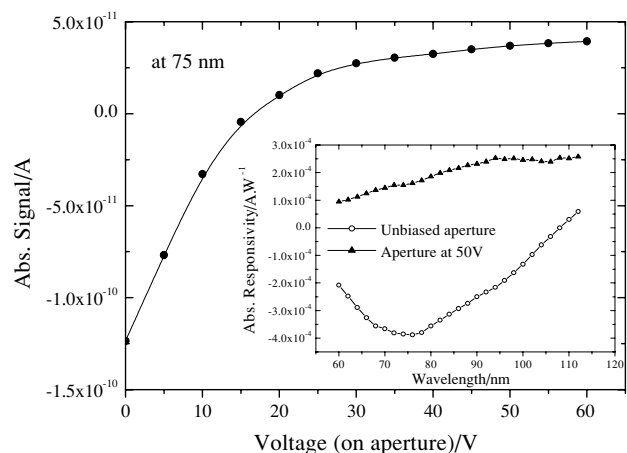


Figure 4. The absolute signal of PIN8 in amperes at 75 nm (current measured with electrometer A1) versus the metallic aperture voltage. The inset shows the absolute spectral response (in A W^{-1}) of PIN8 between 60 nm and 115 nm with a 50 V aperture bias.

aperture. New device architectures are under development to avoid collecting the photo-emitted electrons and increase the homogeneity of the PIN devices (cf 3.4).

The variation of the signal with temperature was also investigated. Thermal cycles (between $-50 \text{ }^\circ\text{C}$ and $+25 \text{ }^\circ\text{C}$) have been performed and the signal at 200 nm wavelength shows a variation of less than $1 \text{ pA } ^\circ\text{C}^{-1}$ following the temperature evolution ($0.1 \text{ }^\circ\text{C}$ steps) with no hysteresis when repeated. The performance of the detector does not change after the thermal cycle.

3.2. Signal stability

The stability of the responsivity under irradiation over prolonged periods is a mission goal for a solar instrument such as LYRA. The signal stability was measured at 1 nm for PIN11 and 12 and at 200 nm wavelength for PIN7 as shown in figure 5. In order to characterize the temporal response of the detectors, the beamline shutter was opened and closed approximately every 1000 s. As seen in the figure, PIN devices show a good stability over a wide temporal range with a negligibly small room temperature background detrapping current of approximately $4 \times 10^{-13} \text{ A}$. This variation is insignificant in absolute terms. The fact that the PIN diode operates in unbiased mode (i.e. it does not require an external voltage) implies a very low dark current. To adjust the incident photon flux at the NI beamline, we used aperture stops of different diameters which cut the beam to a certain percentage of the full beam (approximately 50%, 24%, 12%, 3% and 1%). It can be observed (figure 5, right panel) that PIN7 responds quickly to the signal change and returns to its initial dark signal values after short cycle times irradiation.

3.3. Linearity with photon flux

The linearity of PIN7, 11 and 12 has been investigated over three orders of magnitude (from 1 nW to $1 \mu\text{W}$) using different aperture stops to reduce the radiant power to the lowest measurable values (minimum 1% of the full beam power) or by varying the exit slit of the monochromator. It should be

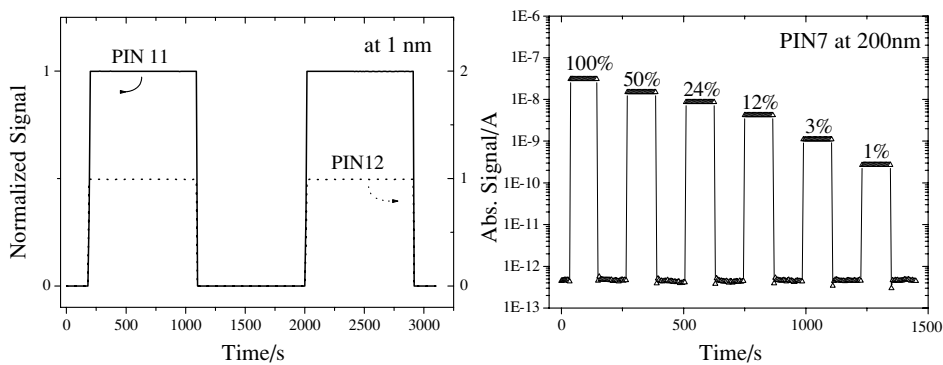


Figure 5. Normalized signal as a function of time for PIN11 and 12 (left) at 1 nm ($\sim 1 \mu\text{W}$ radiant power). On the right, the absolute signal of PIN7 in amperes at 200 nm ($\sim 1.2 \mu\text{W}$ radiant power) as a function of time for different percentages of the full beam. The lines are guides for the eye.

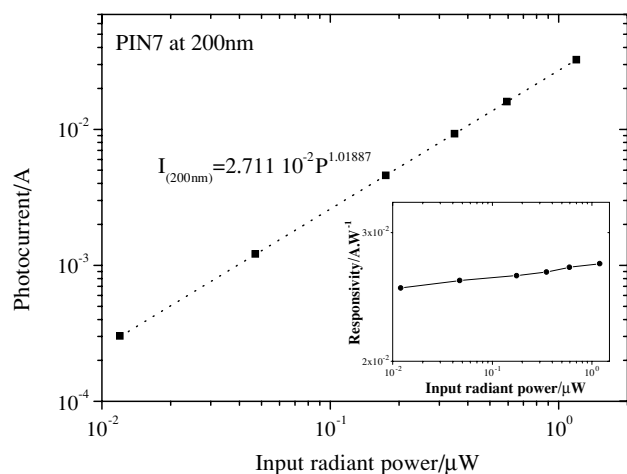


Figure 6. Flux linearity of PIN7 (photocurrent versus incident power) at 200 nm with the fitted function $I = aP^b$. The inset shows the responsivity as a function of the incident radiant power at 200 nm. The lines are guides for the eye.

noted that the expected radiant power in the different LYRA channels is small, typically between 10 and 100 nW during the whole lifetime of the mission. The absolute input radiant power was determined for each aperture by direct comparison with a calibrated PTB reference photodiode. Figure 6 shows the linearity with photon flux of PIN7 at 200 nm wavelength. In this spectral region, the PIN detectors are slightly nonlinear with photon flux. We used a power law $I = aP^b$ to fit the data for PIN7 at 200 nm. The fitted parameters are $a = 0.02711 \pm 0.00002 \text{ A W}^{-1}$ and $b = 1.01887 \pm 0.00133$ which imply a slightly superlinear dependence of the output signal on the incident power ($b = 1$ for linear response). Note that the responsivity of PIN photodiodes at 200 nm increases with increasing incident light power (see inset in figure 6) while for MSM diamond photoconductors [3] the responsivity decreases with input power ($R \propto P^{b-1}$ and $b < 1$).

A possible explanation of this superlinearity is the saturation of traps (i.e. recombination centres) by the photocurrent, i.e. a higher photocurrent results in less active traps and thus longer lifetime and greater charge collection [12–14].

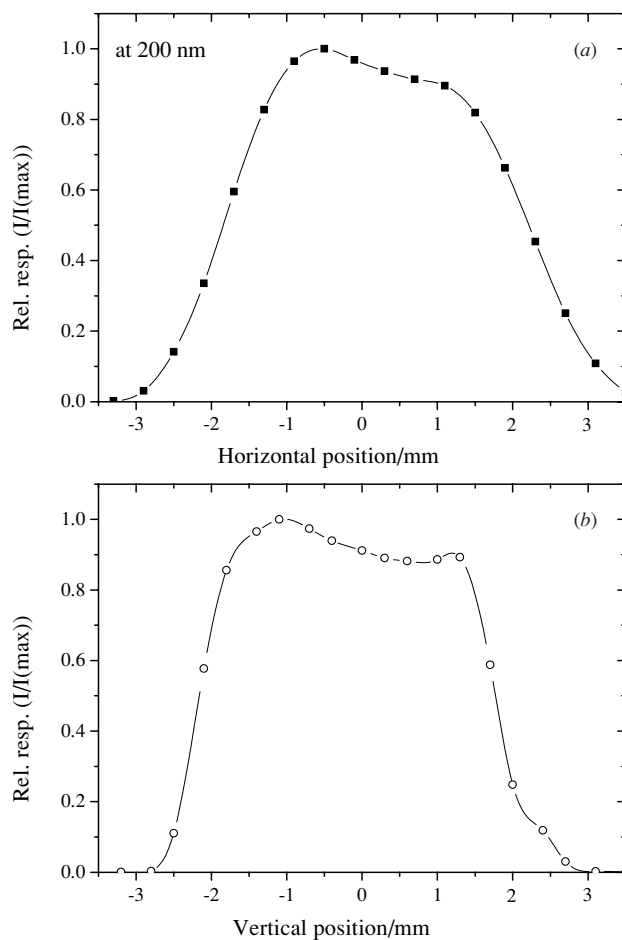


Figure 7. Relative homogeneity of responsivity (linear scan) of PIN7 at 200 nm: (a) along the horizontal position and (b) along the vertical position. The lines are guides for the eye.

3.4. Homogeneity of responsivity (flat field)

The lateral homogeneity of the response (‘flat-field’) of the PIN photodiodes was tested at different wavelengths. At PTB/Bessy II, the detector calibration chambers at the end of the beamline allow the sample to be moved along three axes relative to the beam axis in ultrahigh vacuum. Figures 7(a) and 7(b) show the horizontal and vertical line scans from the centre of the detector of the response of PIN7 at 200 nm

incident wavelength. The relative responsivity maps were built by normalizing the current to its maximum value to aid comparison. The impact of the full beam size (2 mm horizontal and 1 mm vertical at the NI beamline) on the measured profile must be taken into account. The homogeneity of the PIN photodiodes seems to be good with a 5% to 10% deviation observed due to the thick Al layer for the n-contact electrode (see figure 1).

4. Conclusions

In summary, new diamond PIN photodiodes with a photosensitive surface area of 13.85 mm² (Ø 4.2 mm) have been fabricated. The responsivity, stability, linearity and homogeneity have been tested before the final selection of flight model detectors for the solar mission LYRA. The responsivity has been characterized thoroughly in the wavelength range from 1 nm to 1.1 µm. PIN detectors, only used for the Herzberg channel (200–220 nm) due to the high response there, show a sharp diamond band edge around 225 nm and indicate a visible rejection ratio (200 nm versus 500 nm) of six orders of magnitude. In the wavelength range of interest, PIN photodiodes are reasonably homogeneous, linear and stable under brief irradiation. For LYRA, the requirements are radiation hardness, solar blindness, high sensitivity and fast response, good uniformity, good linearity and dynamic range, temperature and long-term stability, and low intrinsic dark current and noise. Diamond photodetectors have high potential to reach all these specifications.

Acknowledgments

The authors acknowledge the support from the Belgian Federal Science Policy Office through the ESA-PRODEX programme. ABM gratefully acknowledges the help of Dr A Debray, Dr E Lebrasseur and Dr E Leclerc. KH is a postdoctoral fellow of the Research Foundation–Flanders (FWO–Vlaanderen).

References

- [1] Hochedez J-F *et al* 2006 LYRA: the solar UV radiometer aboard the ESA PROBA-2 *Adv. Space Res.* **37** 303–12
- [2] Hochedez J-F *et al* 2001 Diamond UV detectors for future solar physics missions *Diamond Relat. Mater.* **10** 673–80
- [3] BenMoussa A *et al* 2005 Performance of diamond detectors for VUV applications *Nucl. Instrum. Methods* at press
- [4] Richter M, Hollandt J, Kroth U, Paustian W, Rabus H, Thornagel R and Ulm G 2001 The two normal-incidence monochromator beam lines of PTB at BESSY II *Nucl. Instrum. Methods* **467–468** 605–8
- [5] Scholze F, Beckhoff B, Brandt G, Fliegauf R, Klein R, Meyer B, Rost D, Schmitz D and Veldkamp M 2000 The new PTB-beamlines for high accuracy EUV reflectometry at BESSY II *Proc. SPIE* **4146** 72–82
- [6] BenMoussa A, Schühle U, Haenen K, Nesládek M, Koizumi S and Hochedez J F 2004 Pin diamond detector development for LYRA, the solar VUV radiometer on board PROBA II *Phys. Status Solidi a* **201** 2536–41
- [7] Richter M, Hollandt J, Kroth U, Paustian W, Rabus H, Thornagel R and Ulm G 2003 Source and detector calibration in the UV and VUV at BESSY II *Metrologia* **40** S107–10
- [8] Scholze F, Tümmler J and Ulm G 2003 High-accuracy radiometry in the EUV range at the PTB soft x-ray beamline *Metrologia* **40** S224–8
- [9] Kania D R, Landstrass M I and Plano M A 1993 Diamond radiation detectors *Diamond Relat. Mater.* **2** 1012–9
- [10] Saito T 2003 Difference in the photocurrent of semiconductor photodiodes depending on the polarity of current measurement through a contribution from the photoemission current *Metrologia* **40** S159–62
- [11] Saito T and Hayashi K 2005 Spectral responsivity measurements of photoconductive diamond detectors in the vacuum ultraviolet region distinguishing between internal photocurrent and photoemission current *Appl. Phys. Lett.* **86** 122113
- [12] Rose T 1955 *Phys. Rev.* **97** 322
- [13] Schaefer R, Zalewski E F and Geist J 1983 Silicon detector nonlinearity and related effects *Appl. Opt.* **22** 1232–5
- [14] Ferrero A, Campos J, Pons A and Corrons A 2005 New model for the internal quantum efficiency of photodiodes based on photocurrent analysis *Appl. Opt.* **44** 208–16